HMG Advance Access published January 13, 2017

Novel *GNB1* mutations disrupt assembly and function of G protein heterotrimers and cause global developmental delay in humans

Katja Lohmann[1,*,#], Ikuo Masuho[2,*], Dipak N. Patil[2], Hauke Baumann[1], Eva Hebert[1], Sofia Steinrücke[1], Daniel Trujillano[3], Nickolas K. Skamangas[2], Valerija Dobricic[4], Irina Hüning[5], Gabriele Gillessen-Kaesbach[5], Ana Westenberger[1], Dusanka Savic-Pavicevic[6], Alexander Münchau[1], Gabriela Oprea[3], Christine Klein[1], Arndt Rolfs[3,7,+], Kirill A. Martemyanov[2,+]

1 Institute of Neurogenetics, University of Lübeck, 23538 Lübeck, Germany

2 Department of Neuroscience, The Scripps Research Institute, Jupiter, FL 33458, USA

3 Centogene AG, 18057 Rostock, Germany

4 Neurology Clinic, University of Belgrade, 11000 Belgrade, Serbia

5 Institut für Humangenetik, Universität zu Lübeck, 23538 Lübeck, Germany

6 Centre for Human Molecular Genetics, Faculty of Biology, University of Belgrade, Belgrade, Serbia

7 Albrecht Kossel Institute for Neuroregeneration, University Hospital Rostock, 18057 Rostock, Germany

* These two authors contributed equally to the study and wish to be recognized as joint first authors.

+ These two authors contributed equally to the study and wish to be recognized as joint last authors.

Corresponding author: Professor Katja Lohmann, PhD

Institute of Neurogenetics, University of Lübeck,

Maria-Goeppert-Str.1, 23562 Lübeck, Germany

Phone: +49-451-31018209; Fax: +49-451-31ß18204; email: katja.lohmann@neuro.uni-luebeck.de

Acknowledgements: This study was supported by NIH grants (NS081282, HL105550, to KM), the German Ministry of Education and Research (BMBF, DYSTRACT consortium, 01GM1514B, to AM, CK, and KL), the Ministry of Education, Science and Technological Development, Republic of Serbia (grant no. 173016, 175090 to VD). CK is a recipient of a career development award from the Hermann and Lilly Schilling Foundation. None of the authors has any conflict of interest.

Abstract

Global developmental delay (GDD), often accompanied by intellectual disability, seizures and other features is a severe, clinically and genetically highly heterogeneous childhood-onset disorder. In cases where genetic causes have been identified, *de-novo* mutations in neuronally expressed genes are a common scenario. These mutations can be best identified by exome sequencing of parent-offspring trios. *De novo* mutations in the guanine nucleotide-binding protein, beta 1 (*GNB1*) gene, encoding the Gβ1 subunit of heterotrimeric G proteins, have recently been identified as a novel genetic cause of GDD. Using exome sequencing, we identified 14 different novel variants (2 splice site, 2 frameshift, and 10 missense changes) in *GNB1* in 16 pediatric patients. One mutation (R96L) was recurrently found in three ethnically diverse families with an autosomal dominant mode of inheritance. Ten variants occurred *de novo* in the patients. Missense changes were functionally tested for their pathogenicity by assaying the impact on complex formation with Gγ and resultant mutant Gβγ with Gα. Signaling properties of G protein complexes carrying mutant Gβ1 subunits were further analyzed by their ability to couple to dopamine D1R receptors by real-time Bioluminescence Resonance Energy Transfer (BRET) assays. These studies revealed altered functionality of the missense mutations R52G, G64V, A92T, P94S, P96L, A106T, and D118G but not for L30F, H91R, and K337Q. In conclusion, we demonstrate a pathogenic role of *de novo* and autosomal dominant mutations in *GNB1* as a cause of GDD and provide insights how perturbation in heterotrimeric G protein function contributes to the disease.

Introduction

Severe, early onset disorders such as intellectual disability (ID) and global developmental delay (GDD) impact on reproductive fitness and are often caused by *de-novo* mutations that can be best identified by next generation sequencing of parent-offspring trios (1). Recently, *de-novo* mutations in the guanine nucleotide-binding protein, beta 1 (*GNB1*) gene have been identified as a novel genetic cause of developmental delay (2). Among the first 13 patients, a wide range of additional symptoms and signs were reported including hypotonia in 11 and seizures in 10 of the patients (2). *GNB1* encodes the guanine nucleotide-binding protein subunit beta-1, $G\beta_1$, a G protein that is involved in signal transduction and forms a heterotrimer complex with Gα and Gγ subunits (3).

With the advent of next generation sequencing, challenges for the detection of disease-causing mutations have changed (4). In the era of Sanger sequencing, the experimental efforts were enormous to detect *one* likely pathogenic variant in sometimes hundreds of successively sequenced candidate genes. Nowadays, nearly all human genes can be sequenced in parallel by exome sequencing with data interpretation, i.e. to find *the* disease causing-mutation among thousands of variants, being the greatest challenge. Even when focusing on rare variants (minor allele frequency <0.01) that are predicted to change the protein sequence (such as missense, nonsense, frameshift, or splice site alterations), there is typically more than one possible disease-causing variant per patient (5). In addition, not all rare and protein-changing variants in a given disease gene are necessarily pathogenic requiring functional characterization of such changes (6).

For signaling molecules, functional impact can be determined by analyzing their interaction with protein partners in the transmission cascade as well as by the ability to propagate receptor-initiated signal. In the case of Gβ, the functionality of wildtype and mutant protein can be investigated by studying its ability to interact with Gγ and Gα subunits and to undergo receptor-driven rearrangements. Changes in these interactions can be monitored *in vitro* by Bioluminescence Resonance Energy Transfer (BRET) between fluorescent-tag labelled components of the cascade. This strategy has proven useful in evaluating the pathogenicity of variants in the *GNAL* gene encoding the Gα subunit in the Gαβγ complex that mediates signaling of the D1 dopamine receptor (D1R), linking this deficiency to a form of adult-onset dystonia (7, 8).

Here, we report 14 novel variants in *GNB1* including 10 missense changes which were assessed for trimeric G protein complex formation and signaling by BRET-based cellular assays to characterize their functional impact. These revealed that only 7 of the 10 missense variants altered functionality, suggesting that the remaining three substitutions represent possibly benign changes.

Results

Genetic analysis

We identified 16 carriers of 14 different rare variants including two frameshift, two splice site, and 10 missense changes (Table 1). Most of these variants (n=8) were located in Exon 7 or its splice sites (Figure 1). Only the recurrent substitution, p.R96L, was shown to be inherited in an autosomal dominant manner. For 10 of the variants a *de-novo* origin could be confirmed since the change was not found in either of the parents. Mode of inheritance could not be determined for three variants due to lack of parental DNA samples and unknown family history (Table 1). All 14 variants were detected in patients and were absent in 4,361 in-house exome datasets at Centogene AG (Rostock, Germany). Further, none of the changes was reported in public databases such as the 60,706 exomes of the Exome Aggregation Consortium (ExAC, http://exac.broadinstitute.org/gene/ENSG00000078369) except for L30F that was found in 2 of ~8,000 South Asian individuals (http://exac.broadinstitute.org/variant/1-1749284-G-A).

First symptoms were noted in the patients at a mean age of 5.3±2.8 years (range: 1-12 years) and nine patients were male. Patients were of diverse ethnic background including Arabic, South Asian, European, and Hispanic (Table 1). All variants were found among about 4,500 individuals referred for genetic testing by exome sequencing at Centogene AG (Rostock, Germany) but neither among the 51 German patients with epilepsy and ID nor among the 40 Serbian Rett-like patients.

Interaction of $G\beta_1$ with $G\alpha$ and $G\gamma$ proteins and propagation of D1R signaling

For the 10 *GNB1* missense variants, we examined the functional effects on D1R signaling via $G\alpha_{olf}\beta_1\gamma_7$. First, we determined the impact on the ability of $G\beta_1$ to form constitutive dimers with the $G\gamma_7$ subunit by bimolecular fluorescence complementation (BiFC) (9) (Figure 2A). $G\gamma_7$ was chosen for its dominant role in mediating $G\alpha_{olf}$ signaling in the striatum (10), a key brain region involved in a wide range of pathologies prominently including movement disorders (11, 12). In this assay, productive formation of a complex between $G\gamma_7$ and $G\beta_1$ reconstitutes Venus protein, detected by its fluorescence. We found that G64V and A106T mutants significantly diminished Venus intensity (Figure 2B). These two mutants also exhibited lower expression levels when analyzed by Western blotting (Figure 2C), suggesting deficits in stability and $G\beta\gamma$ dimer formation. All other

$G\beta_1$ mutants exhibited normal expression and dimerization with $G\gamma_7$ comparable to wild-type construct (Figure 2C).

Second, we investigated the impact of missense changes on the association of $\beta_1\gamma_7$ with $G\alpha_{olf}$ using a cell-based BRET assay (Figure 2D). In this assay, interaction of Venus-tagged $G\beta_1\gamma_7$ dimer with the luciferase-tagged GRK reporter results in a BRET signal. When introduced, $G\alpha_{olf}$ competes with GRK-based reporter for Venus- $G\beta_1\gamma_7$ binding which lowers the BRET signal indicating productive $G\alpha_{olf}$-$\beta_1\gamma_7$ trimer formation (Figure 2D, E). We detected lower basal BRET ratios for G64V and A106T, the mutants with disturbed $G\beta\gamma$ dimer formation, and a milder decrease for P94S and R96L (Figure 2F). The A92T mutant showed higher basal BRET signal, also pointing to deficits in heterotrimer assembly (Figure 2F).

Third, we examined the mutants for their ability to propagate the signal upon stimulation of D1R using an extended cell-based BRET assay (Figure 2G) by monitoring increases in agonist-induced BRET. Stimulation of D1R with agonist dissociates the $G\alpha_{olf}$-$\beta_1\gamma_7$ trimer, leading to a rapid increase in BRET signal, which serves as a measure for the functional activity of $G\beta_1\gamma_7$ (Figure 2G, H). We found that in addition to deficient mutants (G64V, A92T, P94S, R96L, A106T), two other substitutions (R52G and D118G) showed significantly lower response amplitudes, suggesting deficits in receptor-driven G protein activation (Figure 2I, J). In an additional control experiment, we examined basal BRET signal and Venus intensity of $G\beta_1$ mutants in the absence of $G\alpha$ subunit (Supplemental Figure 1). We found correlation of these two measurements, indicating that all $G\beta_1$ mutants maintained association with the GRK3-based reporter proportionately scaling according to their expression level. Thus, we concluded that the deficiency observed in functional analysis cannot be explained by the loss of reporter binding. Of note, we detected normal behavior indistinguishable from wildtype $G\beta_1$ for three of the variants including L30F, H91R, and K337Q by all three measures (Figure 2B, F, I).

Finally, we investigated the 3D structure of the G protein heterotrimer containing $G\beta_1$ and the location of identified variants (Figure 3). This revealed that the amino acid residues G64 and A106 are located close to each other within the inner β-propeller structure (Figure 3B). Further, amino acid residues R52, A92, P94, P96, and D118 are located close to interaction sites with $G\alpha$ or effector molecules (Figure 3C, D). In contrast, the likely benign variants L30F, H91R, and K337Q are more distantly located from these interaction sides (Figure 3D).

Clinical findings in patients with pathogenic mutations

Based on the results of the functional studies in the BRET assays, the missense variants R52G, G64V, A92T, P94S, R96L, A106T, and D118G lead to a loss of function and thus can be considered as disease-causing (Figure 1). In addition, we interpreted the splice-site and frameshift variants identified in four patients to be pathogenic, as well, because of the predicted complete loss of functional protein. These 11 changes were present in 13 patients who had a mean age at diagnosis of 5.0±2.8 years (range: 1-12 years) and all had GDD. Among these, 10 patients (87%) were diagnosed with ID. Seizures were reported in 7 (54%), nystagmus in 6 (46%), muscular hypotonia in 5 (38%), and ophthalmoplegia in 4 (31%) patients. In addition, abnormal myelination, craniosynostosis, and cerebellar hypoplasia were observed in 5, 3, and 2 patients, respectively. Ataxia was noted in 4, chorea and dystonia (13) in one patient each (Table 1). Of note, the age at diagnosis and the phenotypic presentation did not vary between patients with functionally proven mutations and variants of unknown significance, except for the absence of GDD in the patient with the L30F variant.

Discussion

Here, we present clinical findings on 16 carriers of 14 different rare, protein-changing variants in *GNB1*. Most of these changes occurred *de novo* and have not been reported previously. *GNB1* encodes the G protein subunit $G\beta_1$ which requires forming heterotrimers with Gα and Gγ subunits for function as a transducer of signals from G protein-coupled receptors. It has previously been noted that many of the reported *GNB1* mutations are located at the interface of Gβγ and Gα (2) based on the crystal structure of the heterotrimer.

To differentiate between likely pathogenic and benign missense variants (14), we investigated the effects of the mutations on G protein heterotrimer formation and its ability to mediate D1R signaling using live-cell BRET assays. In addition, we modeled the 3D structure of respective protein complexes and evaluated the location of the variants in these assemblies. First, we tested Gβ and Gγ dimer formation by BiFC and demonstrated deficits in Gβγ dimer formation through G64V and A106T mutations. Since the amino acid residues G64 and A106 are buried in the β-propeller structure (Figure 3A, B), it is likely that introducing larger side chains by the mutations disrupt the structural integrity impeding Gβ1 folding. Indeed, Western blot analysis showed low expression of these mutants (Figure 2C). Next, we investigated the effects of mutations on the ability of trimeric G_{olf} to propagate D1R signal by cell-based BRET assays. As expected from the observed deficits in protein expression, G64V and A106T mutants showed a low basal BRET ratio and small agonist-induced BRET response (Figure 2F, I, J). A similar, yet milder decrease in basal BRET ratio was also observed for the P94S and R96L mutants suggesting increased binding to $G\alpha_{olf}$ (Figure 2F, J). Although the region encompassing P94 and R96 is known

to be involved in interactions with the effector molecules (15) (Figure 3D, upper panel), we found no deficiency in GRK3 binding (Supplemental Figure 1). Accordingly, we speculate that these mutations enhance $G\beta_1\gamma_7$'s ability to interact with Gα subunit, lowering basal BRET ratio and agonist-induced BRET response. In contrast, the A92T mutant showed high basal BRET signal (Figure 2E, I), suggesting deficits in association with $G\alpha_{olf}$. Indeed, the neighboring residue K89 is known to be essential for stabilizing Gαβγ trimer through a tripartite interaction with the N-terminal helix of Gα subunit (16) (Figure 3C, lower panel). Preservation of GRK binding to A92T $G\beta_1$ suggests a selective role of A92 in discriminating between Gα and effector interactions. Therefore, we speculate that the A92T mutation likely produces constitutively active Gβγ dimer. This is expected to possibly result in a gain-of-function in engaging Gβγ effectors, similarly to what has been reported for several GNB1 mutations linked to diverse human tumors (17). However, elevation of the baseline at rest also diminishes the extent of the receptor mediated signaling and thus the pathological effect of this mutation could still be originating from the loss-of-function as far as transduction of neurotransmitter signals is concerned. Finally, when using agonist-induced BRET, we demonstrated lower response amplitudes for R52G and D118G in addition to the above-mentioned five missense variants with lower basal BRET signal. This may be caused by deficits in agonist-induced G protein activation. Notably, these residues surround the Gα binding interface and thus likely play a role in receptor-induced re-arrangement (Figure 3C, upper panel). In contrast, the likely benign variants L30F, H91R, and K337Q that did not show any differences in behavior compared to wildtype $G\beta_1$ in the BRET assays, are more distantly located from interaction sides with Gα or effector molecules (Figure 3D).

Thus, we conclude that only 7 of the 10 missense mutations found in patients in this study are likely pathogenic due to altered Gβ1 functionality. In addition, the two splice site mutations affecting the conserved last intronic base pair at the acceptor splice site of Introns 6 and 10, respectively, likely lead to a splicing defect and subsequent degradation of the erroneous RNA by nonsense-mediated decay. The two frameshift mutations are also considered to result in a premature stop codon, similarly leading to haploinsuffiency. Of note, we did not observe any obvious correlation between altered behavior of the mutations in the functional assays and the clinical phenotypes. In this context, it is also worth noting that the degree of functional alterations *in vitro* may not fully reflect the situation *in vivo* since we tested in our model system functionality of *one* multimeric complex in response to a single signal molecule and a single effector protein. Along the same lines, although, we did not observe any effect for L30F, H91R, and K337Q in the assays that we used, it is still conceivable that these variants may impact $G\beta_1$ function, i.e. reactions that were not tested in our experiments such as interactions with other effector proteins and/or other α and γ subunits, and thus may still be causative for the disease in the respective carriers. However, our structural modeling indicates that these amino acid substitutions are not located

at the common protein interaction interface of $G\beta_1$, making this possibility less likely. Further, L30F has been reported in two individuals who are free of severe pediatric disease in ExAC (http://exac.broadinstitute.org/about) also suggesting that it represents a rare but benign variant. In agreement with these considerations, the patient carrying the L30F variant did – unlike all other patients - not present with GDD.

Combining the previously published (2) and the present study, almost 30 carriers of germline mutations in *GNB1* have been identified to date. The mutation frequency (<0.5%) is low and consistent in both studies which included >10,000 exomes of individuals with various undiagnosed, likely genetic disorders (5,866 in (2) and 4,377 in our in-house database). Thus, it is not unexpected that we did not observe another *GNB1* mutation carrier among the almost 100 additional patients that we screened for mutations by conventional Sanger sequencing in a candidate-based approach.

Phenotypically, GDD was present in all 26 mutation carriers (including only the functionally confirmed ones from our study). Frequent symptoms that were present in more than half of the reported patients include seizures (17/26), muscular hypotonia (17/26), ophthalmological disorder (17/26), and ID (14/26). Although abnormalities on brain MRI were only reported in 12 of the patients (46%), this frequency is probably an underestimate since not all patients underwent MRI and several were still very young (<1 year, (2)) at the time of examination. Growth delay was reported in 9 (35%) and movement disorders including tics, ataxia, dystonia, or chorea were noticed in at least 9 patients. This illustrates that the phenotypic spectrum in *GNB1* mutation carriers seems to be broad and additional signs and symptoms may be part of the clinical spectrum. For our patients, the clinical information was limited and re-examination of mutation carriers was not possible, except for one patient who was reported in detail previously (13).

Taken together, our study further underlines the importance and power of exome sequencing, especially in genetically highly heterogeneous disorders such as GDD and ID. None of the at least 13 mutation carriers was identified in a candidate-based analysis of about 100 patients with a similar phenotype. Although the detection of a *GNB1* mutation in an affected individual currently does not influence treatment choices and no causative therapy is available as yet, it reduces uncertainty in the families by establishing a diagnosis (18) and has a major influence on genetic counseling and family planning since almost all of the mutations occurred *de novo*.

Materials and Methods

Exome sequencing

Exome sequencing was carried out at Centogene AG (Rostock, Germany) according to standard diagnostic procedures. Prior to exome sequencing, all participants gave written informed consent. In brief, genomic DNA was extracted from whole blood. Exome capture was carried out with Illumina's Nextera Rapid Capture Exome Kit followed by massively parallel sequencing on a NextSeq500 Sequencer (Illumina, San Diego, CA, USA). Raw sequencing reads were converted to fastq format using bcl2fastq software (Illumina). Using an in-house developed pipeline for exome data analysis, the reads were aligned to the human reference genome (GRCh37, hg19 build) using bwa software with the mem algorithm. Alignments were converted to binary bam file and variant calling was performed using three different variant callers (GATK HaplotypeCaller, freebayes and samtools). Variants were annotated using Annovar and in-house ad hoc bioinformatics tools. All data were fed into an in-house database that was searched for rare (frequency in publically available and the in-house database <0.01) and protein-changing variants in *GNB1*.

Mutational analysis by Sanger sequencing

The study was approved by the ethics committee at the University of Lübeck (Germany). For mutational analysis of *GNB1* as a candidate gene, we Sanger sequenced all 9 coding exons of *GNB1* (NM_001282539) in a total of 91 patients. This included 51 unrelated, mainly German patients (21 male, mean age: 14.4±11.1 years, age range 2–50 years) with a combination of epileptic seizures, psychomotor retardation, and ID with delayed speech development. These patients had previously been tested negative for mutations in *SCN2A* (19). Further, we included 40 patients with a clinical presentation of Rett syndrome who were diagnosed from 2002 to 2015 (37 females, mean age: 10.2±4.0 years (range: 4–20 years). Mutations in *MECP2* were previously excluded in these patients.

cDNA Constructs and antibodies

Dopamine D1 receptor and $G\alpha_{olf}$ in pcDNA3.1+ were purchased from the cDNA Resource Center. Plasmids encoding Venus 156-239-Gβ1 was a gift from N. Lambert (Georgia Regents University)(20). Venus 1-155-Gγ7 encodes amino acids 1-155 of Venus fused to a GGSGGG linker at the N-terminus of human Gγ7 (AF493874). Plasmids encoding Flag-Ric-8B were gifts from B. Malnic (University of São Paulo) (21). PTX-S1 was kindly provided by Eitan Reuveny (Weizmann Institute of Science, Rehovot, Israel) (22). masGRK3ct-Nluc were

previously described (23). Venus 156-239-Gβ1 mutants were constructed with site-directed mutagenesis using the QuikChange II® Site-directed Mutagenesis Kit (Agilent Technologies) and Venus 156-239-Gβ1 as a template. All mutations were confirmed in the plasmids by Sanger sequencing. GFP (clones 7.1 and 13.1) and GAPDH (clone 6C5) antibodies were purchased from Roche and Millipore, respectively.

Real-time monitoring of G protein activity by fast kinetic BRET assay

BRET experiments were performed as previously reported with slight modifications (23, 24). Briefly, 293T/17 cells were grown in DMEM supplemented with 10% FBS, minimum Eagle's medium non-essential amino acids, 1 mM sodium pyruvate, and antibiotics (100 units/ml penicillin and 100 µg/ml streptomycin) at 37 °C in a humidified incubator containing 5% CO_2. Cells were transfected with Lipofectamine LTX transfection reagents (12 µl/6-cm dish) and PLUS (7.5 µl/6-cm dish). Dopamine D1 receptor, Gαolf, Venus-156-239-Gβ1, Venus-1-155-Gγ7, Flag-Ric-8B, masGRK3ct-Nluc, and PTX-S1 constructs (total 7.5 µg) were used at a 1:6:1:1:1:1:1 ratio (ratio 1 = 0.42 µg of plasmid DNA). Since promiscuous nature of G protein-coupling of GPCRs are reported (23), PTX-S1 were transfected to inhibit the possible coupling of endogenous Gi/o to D1R. BRET and Venus intensity measurements were performed using a microplate reader (POLARstar Omega, BMG Labtech) equipped with two emission photomultiplier tubes. All measurements were performed at room temperature. The BRET signal is determined by calculating the ratio of the light emitted by Venus-Gβ1γ7 (535 nm) over the light emitted by masGRK3ct-Nluc (475 nm). The average baseline value recorded before agonist stimulation was subtracted from BRET signal values, and the resulting difference (ΔBRET ratio) was plotted as traces.

Western blotting

For each sample, about 5×10^6 cells were lysed in 500 µl of sample buffer [125 mM tris-HCl (pH 6.8), 4 M urea, 4% SDS, 10% 2-mercaptoethanol, 20% glycerol, bromophenol blue (0.16 mg/ml)]. Western blotting analysis of proteins was performed after samples were resolved by SDS–polyacrylamide gel electrophoresis and transferred onto PVDF membranes. Blots were blocked with 5% skim milk in PBS containing 0.1% Tween 20 (PBST) for 30min at room temperature, which was followed by a 90-min incubation with specific antibodies diluted in PBST containing 1% skim milk. Blots were washed in PBST and incubated for 45 min with a 1:10,000 dilution of secondary antibodies conjugated with horseradish peroxidase in PBST containing 1% skim milk. Proteins were visualized on x-ray film by SuperSignal West Femto substrate (Pierce).

Visualization of 3D models of Gαβγ heterotrimers and effector molecule binding

To investigate the 3D structure of the G protein heterotrimer containing Gβ1 and the location of identified variants, we modeled this complex based on the crystal structure of Gαi1β1γ2 (PDB ID: 1GP2) (16) which is one of only two reported crystal structures of G protein heterotrimers. In addition, footprints of Gα and effector molecule GRK binding sites on the molecular surface of Gβ1 were generated. GRK2-Gβ1γ2 complex (PDB ID: 1OMW) (15) and Gαi1β1γ2 (PDB ID: 1GP2) were used to obtain the footprints. Figures (Figure 3) were drawn using PyMOL (http://www.pymol.org/).

Acknowledgements

This study was supported by NIH grants (NS081282, HL105550, to KM), the German Ministry of Education and Research (BMBF, DYSTRACT consortium, 01GM1514B, to AM, CK, and KL), the Ministry of Education, Science and Technological Development, Republic of Serbia (grant no. 173016, 175090 to VD). CK is a recipient of a career development award from the Hermann and Lilly Schilling Foundation.

Conflict of interest statement

None of the authors has any conflict of interest.

References

1 Vissers, L.E., Gilissen, C. and Veltman, J.A. (2016) Genetic studies in intellectual disability and related disorders. *Nat. Rev. Genet.*, **17**, 9-18.

2 Petrovski, S., Kury, S., Myers, C.T., Anyane-Yeboa, K., Cogne, B., Bialer, M., Xia, F., Hemati, P., Riviello, J., Mehaffey, M. *et al.* (2016) Germline De Novo Mutations in GNB1 Cause Severe Neurodevelopmental Disability, Hypotonia, and Seizures. *Am. J. Hum. Genet.*, **98**, 1001-1010.

3 Freissmuth, M., Casey, P.J. and Gilman, A.G. (1989) G proteins control diverse pathways of transmembrane signaling. *Faseb J.*, **3**, 2125-2131.

4 Lohmann, K. and Klein, C. (2014) Next Generation Sequencing and the Future of Genetic Diagnosis. *Neurotherapeutics*, **11**, 699-707.

5 Gilissen, C., Hoischen, A., Brunner, H.G. and Veltman, J.A. (2012) Disease gene identification strategies for exome sequencing. *Eur. J. Hum. Genet.*, **20**, 490-497.

6 Lohmann, K., Uflacker, N., Erogullari, A., Lohnau, T., Winkler, S., Dendorfer, A., Schneider, S.A., Osmanovic, A., Svetel, M., Ferbert, A. *et al.* (2012) Identification and functional analysis of novel THAP1 mutations. *Eur. J. Hum. Genet.*, **20**, 171-175.

7 Kumar, K.R., Lohmann, K., Masuho, I., Miyamoto, R., Ferbert, A., Lohnau, T., Kasten, M., Hagenah, J., Bruggemann, N., Graf, J. *et al.* (2014) Mutations in GNAL: a novel cause of craniocervical dystonia. *JAMA Neurol.*, **71**, 490-494.

8 Fuchs, T., Saunders-Pullman, R., Masuho, I., Luciano, M.S., Raymond, D., Factor, S., Lang, A.E., Liang, T.W., Trosch, R.M., White, S. *et al.* (2013) Mutations in GNAL cause primary torsion dystonia. *Nat. Genet.*, **45**, 88-92.

9 Hu, C.D. and Kerppola, T.K. (2003) Simultaneous visualization of multiple protein interactions in living cells using multicolor fluorescence complementation analysis. *Nat. Biotechnol.*, **21**, 539-545.

10 Schwindinger, W.F., Mihalcik, L.J., Giger, K.E., Betz, K.S., Stauffer, A.M., Linden, J., Herve, D. and Robishaw, J.D. (2010) Adenosine A2A receptor signaling and golf assembly show a specific requirement for the gamma7 subtype in the striatum. *J. Biol. Chem.*, **285**, 29787-29796.

11 Corvol, J.C., Muriel, M.P., Valjent, E., Feger, J., Hanoun, N., Girault, J.A., Hirsch, E.C. and Herve, D. (2004) Persistent increase in olfactory type G-protein alpha subunit levels may underlie D1 receptor functional hypersensitivity in Parkinson disease. *J. Neurosci.*, **24**, 7007-7014.

12 Girault, J.A. (2012) Signaling in striatal neurons: the phosphoproteins of reward, addiction, and dyskinesia. *Prog. Mol. Biol. Transl. Sci.*, **106**, 33-62.

13 Steinrucke, S., Lohmann, K., Domingo, A., Rolfs, A., Baumer, T., Spiegler, J., Hartmann, C. and Munchau, A. (2016) Novel GNB1 missense mutation in a patient with generalized dystonia, hypotonia, and intellectual disability. *Neurol. Genet.*, **2**, e106.

14 Richards, S., Aziz, N., Bale, S., Bick, D., Das, S., Gastier-Foster, J., Grody, W.W., Hegde, M., Lyon, E., Spector, E. *et al.* (2015) Standards and guidelines for the interpretation of sequence variants: a joint consensus recommendation of the American College of Medical Genetics and Genomics and the Association for Molecular Pathology. *Genet. Med.*, **17**, 405-424.

15 Lodowski, D.T., Pitcher, J.A., Capel, W.D., Lefkowitz, R.J. and Tesmer, J.J. (2003) Keeping G proteins at bay: a complex between G protein-coupled receptor kinase 2 and Gbetagamma. *Science*, **300**, 1256-1262.

16 Wall, M.A., Coleman, D.E., Lee, E., Iniguez-Lluhi, J.A., Posner, B.A., Gilman, A.G. and Sprang, S.R. (1995) The structure of the G protein heterotrimer Gi alpha 1 beta 1 gamma 2. *Cell*, **83**, 1047-1058.

17 Yoda, A., Adelmant, G., Tamburini, J., Chapuy, B., Shindoh, N., Yoda, Y., Weigert, O., Kopp, N., Wu, S.C., Kim, S.S. *et al.* (2015) Mutations in G protein beta subunits promote transformation and kinase inhibitor resistance. *Nat. Med.*, **21**, 71-75.

18 Lingen, M., Albers, L., Borchers, M., Haass, S., Gartner, J., Schroder, S., Goldbeck, L., von Kries, R., Brockmann, K. and Zirn, B. (2015) Obtaining a genetic diagnosis in a child with disability: impact on parental quality of life. *Clin. Genet.*, **89**, 258-266.

19 Baasch, A.L., Huning, I., Gilissen, C., Klepper, J., Veltman, J.A., Gillessen-Kaesbach, G., Hoischen, A. and Lohmann, K. (2014) Exome sequencing identifies a de novo SCN2A mutation in a patient with intractable seizures, severe intellectual disability, optic atrophy, muscular hypotonia, and brain abnormalities. *Epilepsia*, **55**, e25-29.

20 Hollins, B., Kuravi, S., Digby, G.J. and Lambert, N.A. (2009) The c-terminus of GRK3 indicates rapid dissociation of G protein heterotrimers. *Cell. Signal.*, **21**, 1015-1021.

21 Von Dannecker, L.E., Mercadante, A.F. and Malnic, B. (2006) Ric-8B promotes functional expression of odorant receptors. *Proc. Natl. Acad. Sci. U. S. A.*, **103**, 9310-9314.

22 Raveh, A., Cooper, A., Guy-David, L. and Reuveny, E. (2010) Nonenzymatic rapid control of GIRK channel function by a G protein-coupled receptor kinase. *Cell*, **143**, 750-760.

23 Masuho, I., Ostrovskaya, O., Kramer, G.M., Jones, C.D., Xie, K. and Martemyanov, K.A. (2015) Distinct profiles of functional discrimination among G proteins determine the actions of G protein-coupled receptors. *Sci. Signal.*, **8**, ra123.

24 Masuho, I., Martemyanov, K.A. and Lambert, N.A. (2015) Monitoring G Protein Activation in Cells with BRET. *Methods Mol. Biol.*, **1335**, 107-113.

Legends to Figures

Figure 1. Schematic representation of GNB1 variants. The exons of the *GNB1* gene are shown to scale with the nine coding exons highlighted by boxes and flanked by the respective untranslated regions (UTR). Previously reported mutations (2) are shown above the gene in black and newly identified variants in this study are indicated below the gene including truncating mutations (blue), missense changes which alter the functionality of Gβ1 (red), and likely benign variants (green).

Figure 2. Effect of missense mutations in Gβ1 on Gβγ dimer formation, trimeric G_{olf} formation and agonist-induced G protein activation. A. Schematic presentation of the BiFC assay to test Gβγ dimer formation. Two nonfluorescent fragments of Venus fused to Gβ and Gγ, respectively, are brought together by interactions between Gβ and Gγ and produces a yellow fluorescent protein, Venus. **B**. Quantitative assessment of Gβγ dimer formation of Gβ1 mutants. HEK293T/17 cells were transiently transfected with D1R, $G\alpha_{olf}$, Venus-156-239-Gβ1, Venus-1-155-Gγ7 and effector reporter (masGRK3ct-Nluc), and Venus intensity was measured indicating impaired dimer formation for G64V and A106T. **C.** Western blot analysis of protein expression in HEK293T/17 cells. Cell lysates of the transfected cells used to measure Venus intensity in panel B were subjected to Western blotting. Anti-GFP antibody was used to detect Venus 156-239-Gβ1. Western blotting with anti-GAPDH antibody was performed as a loading control. **D.** Schematic presentation of the experimental set-up to assess basal BRET levels (before agonist application) to test for trimer formation. Expression of masGRK3ct-Nluc with Venus-Gβγ produces GRK3-bound Gβγ-induced increase of Bioluminescence Resonance Energy Transfer (BRET) between Nluc and Venus. Additional expression of the Gα subunit sequestrates Gβγ from masGRK3ct-Nluc. **E**. This additional expression of Gα decreases BRET signal and disruption of αβγ trimer formation increases BRET signal. **F**. Basal BRET ratio for the 10 tested missense changes demonstrated decreased BRET signal for G64V, P94S, R96L, and A106T as well as an increased basal BRET ratio for A92T. **G.** Schematic BRET assay design for monitoring G protein activation. Dopamine stimulation of cells transiently transfected with D1R, $G\alpha_{olf}$ with BRET sensors results in the dissociation of $G\alpha_{olf}$ from the heterotrimer. Released Venus-tagged Gβγ subunits become available for interaction with the masGRK3ct-Nluc reporter, producing the BRET signal. **H**. Upon agonist-induced stimulation (red arrow), the BRET signal increases. **I.** BRET amplitude for the 10 tested missense changes demonstrated decreased BRET signal also for R52G and D118G. **J.** Characterization of mutant Gβ1 subunits by BRET assay. *Trace lines* represent D1R-G_{olf} signaling before (basal BRET) and after agonist application (agonist-induced BRET) to cells transfected with wild type or

mutant Gβ1. Responses to application of dopamine (100 μM) were recorded. Dopamine application is indicated by a red arrow. Expression of all signaling components is required to see an agonist-induced response, indicating the reconstitution of D1R-G_{olf} signaling by exogenous expression of signaling molecules.

Data are means of six replicates. Values represent means ± SEM from three independent experiments each performed with six replicates. One-way ANOVA followed by Dunett's post-hoc test was conducted with GraphPad Prism Ver. 6 (asterisk, $P < 0.05$; double asterisk, $P < 0.01$; triple asterisk, $P < 0.001$, quadruple asterisk, $P < 0.0001$).

Figure 3. Mutant residues of Gβ1 on three-dimensional crystal structures. A. Cartoon representation of crystal structure of the Gαβγ trimer complex with mutations shown in red spheres. Gα, Gβ and Gγ are shown in green, cyan, and blue, respectively. The published crystal structure of Gαi1/Gβ1γ2 (PDB ID: 1GP2) was chosen as a model of the trimer (16). **B.** Mutant residues in Gβ1γ2 dimer found in dystonia patients are highlighted and labeled by red spheres. **C and D.** Binding sites on the molecular surface of Gα (C, green) and GRK (D, yellow) and on Gβ1 (cyan), respectively. Mutations are indicated in red. GRK2-Gβ1γ2 complex (PDB ID: 1OMW) (15) and Gαi1β1γ2 (PDB ID: 1GP2) were used to obtain the footprints. The residue colored in black indicates the overlap residue of the GRK binding site and the R96L mutation. The bird´s eye perspectives are shown at the bottom panels.

Table 1. Clinical, genetic, and functional information of mutation carriers

Case	**1**	**2**	**3**	**4**	**5**	**6**	**7**	**8**	**9**	**10**	**11**	**12**	**13**	**14**	**15**	**16**
Sex	m	f	f	m	m	m	f	m	f	f	m	m	f	m	f	m
Age at diagnosis	4	2.5	4	2.4	5	8	2.9	4	6	1	Unk	8	12	8	6	8
Ethnicity	Saudi Arabian	Qatar	Egypt	Saudi Arabian	Israeli	Mexican	Saudi Arabian	Kuwaiti	Israeli	Indian	Mexican	Algerian	German	Saudi Arabian	Indian	Saudi Arabian
Var Build 19 NM_002074 NP_002065	1:1749284 c.88C>T p.L30F	1:1747244 c.154C>G p.R52G	1:1747207 c.191G>T p.G64V	1:1736021 c.268-1G>T p.?	1:1736013 c.272_275del p.?	1:1736016 c.272A>G p.H91R	1:1736014 c.274G>A p.A92T	1:1736008 c.280C>T p.P94S	1:1736001 c.287G>T p.R96L			1:1735972 c.316G>A p.A106T	1:1735935 c.353A>G p.D118G	1:1720492 c.915_916del p.?	1:1718877 c.917-1G>T p.?	1:1718784 c.1009A>C p.K337Q
Location of mut.	Exon 4	Exon 5	Exon 5	Intron 6	Exon 7	Exon 7	Exon 7	Exon 7	Exon 7			Exon 7	Exon 7	Exon 10	Intron 10	Exon 11
Type of mut.	ms	ms	ms	ss	fs	ms	ms	ms	ms			ms	ms	fs	ss	ms
Change in function	No	Yes	Yes	Not tested	Not tested	No	Yes	Yes	Yes			Yes	Yes	Not tested	Not tested	No
CADD score (v1.3)	22	21	33	27	35	18	25	23	26			24	29	35	26	24
Inheritance	De novo	De novo	De novo	De novo	De novo	Unk	De novo	Unk	Dominant	Dominant	Dominant	De novo	De novo	De novo	Unk	De novo
GDD	no	yes	yes	yes	yes	yes	yes	yes	yes	yes	yes	yes	yes	yes	yes	yes
Growth delay	yes	no	no	no	yes	yes	no	no	yes	no	no	no	no	no	yes	no
Muscular hypotonia	yes	no	no	yes	no	yes	yes	no	no	no	no	no	yes	yes	yes	no
ID	yes	yes	no	yes	yes	yes	yes	yes	no	yes	yes	no	yes	yes	yes	yes
Seizures	yes	no	no	no	yes	yes	yes	no	yes	no	yes	yes	no	yes	yes	yes
Cranniosynostosis	no	no	no	yes	yes	no	no	no	no	no	no	yes	no	no	no	no
Cerebellar hypoplasia	no	yes	no	no	no	yes	yes	no	no	no	no	no	no	no	no	no
Abnormal myelination	no	no	no	yes	yes	no	no	no	yes	no	yes	no	no	yes	no	yes
Ophthalmoplegia	no	yes	no	yes	no	no	no	yes	yes	no	no	no	no	no	no	no
Nystagmus	yes	yes	no	no	yes	yes	no	no	yes	no	yes	no	no	yes	yes	yes
Ataxia	yes	yes	no	no	yes	no	yes	no	no	no	no	no	no	no	yes	no
Chorea	no	no	no	no	no	no	no	yes	no	no	no	no	no	no	no	no
Dystonia	no	no	no	no	no	no	no	no	no	no	no	no	yes	no	no	no

Unk: unknown, ss: splice site; fs. Frameshift, ms: missense; GDD: global developmental delay, ID: intellectual disability, CADD: combined annotation dependent depletion

Abbreviations

BiFC	Bimolecular fluorescence complementation
BRET	Bioluminescence Resonance Energy Transfer
ExAC	Exome Aggregation Consortium
GDD	Global developmental delay
GNB1	guanine nucleotide-binding protein, beta 1
GRK	G protein coupled receptor kinase
ID	Intellectual disability

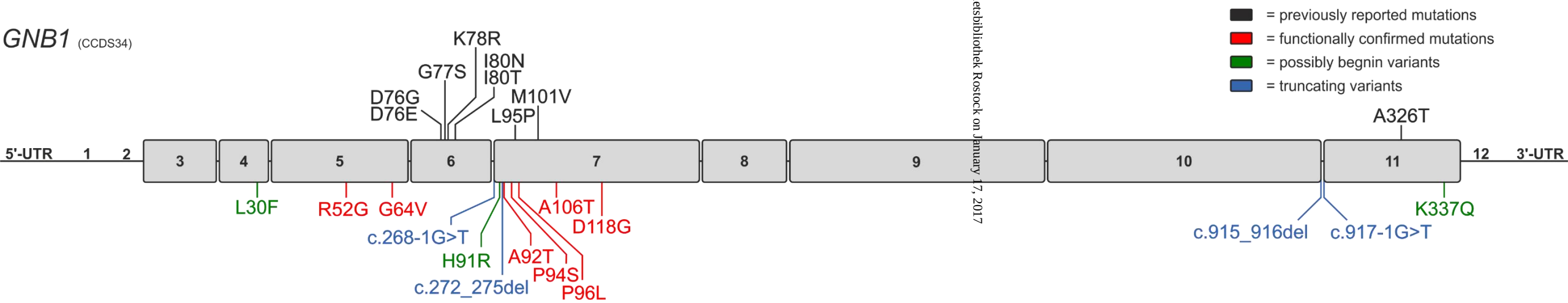

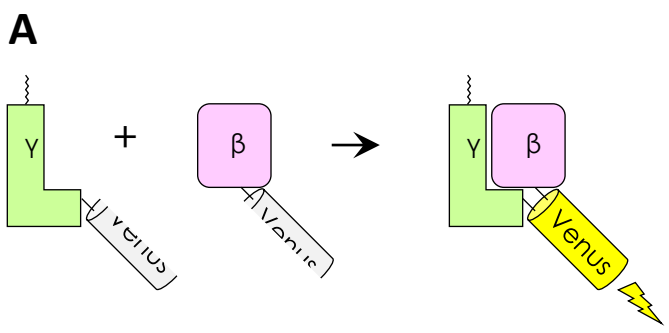

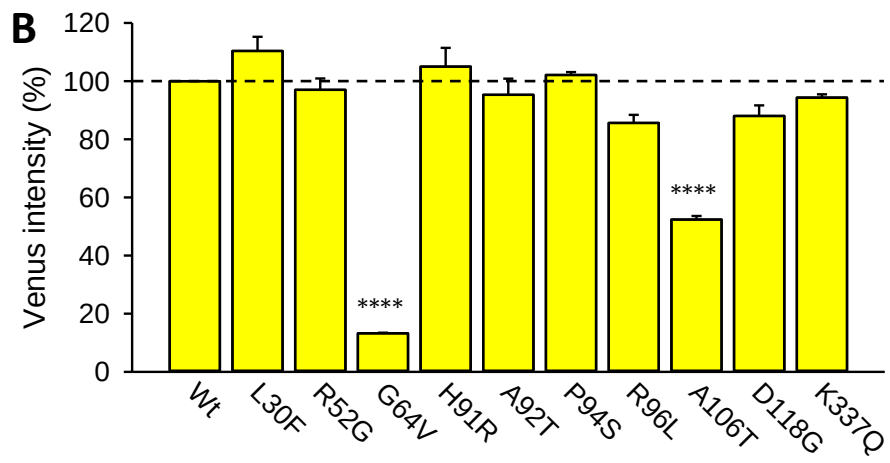

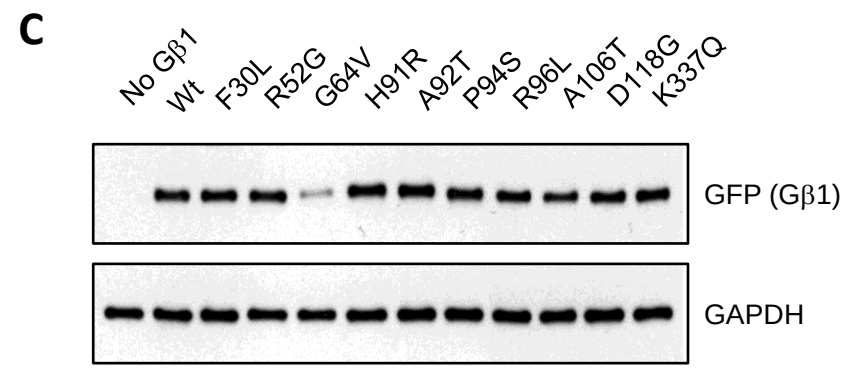

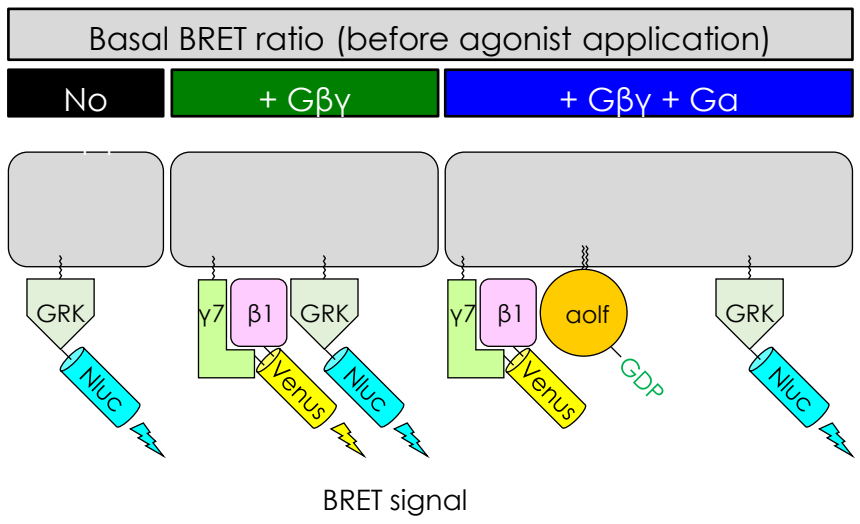

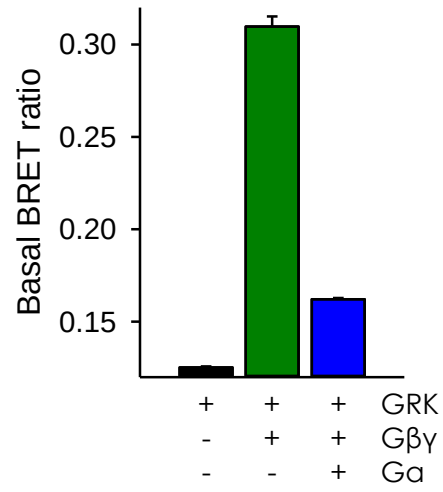

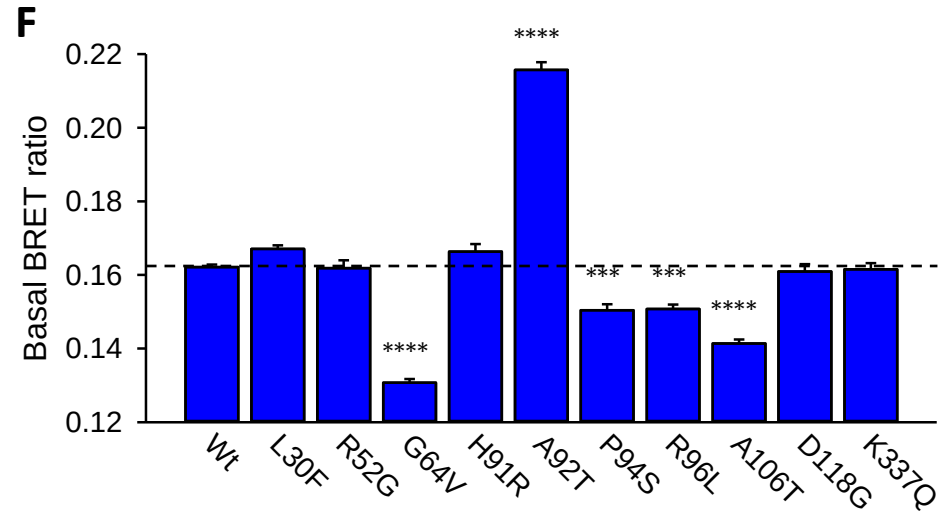

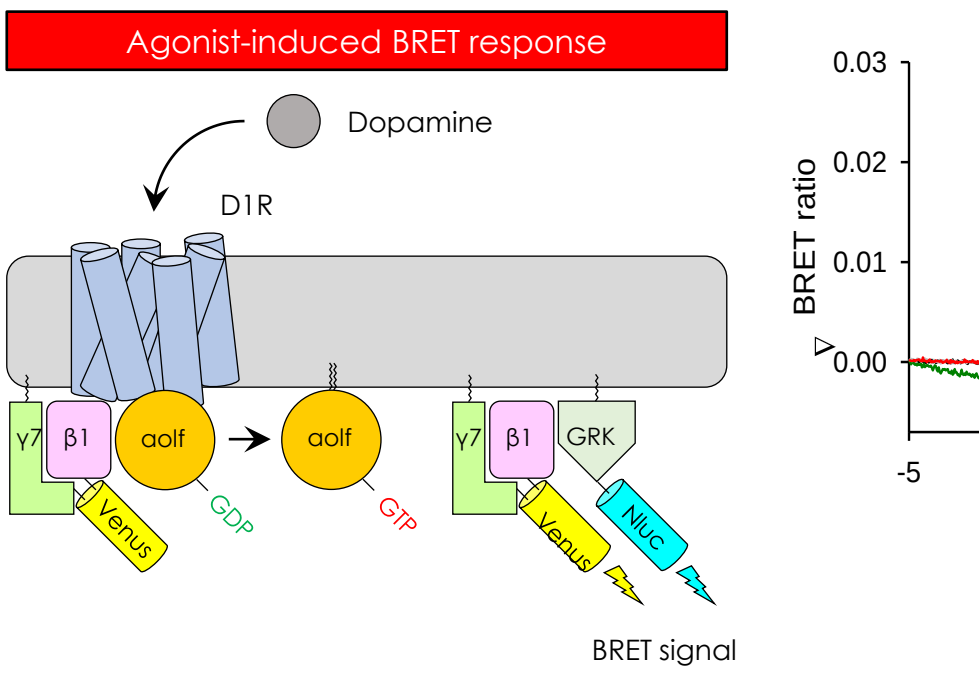

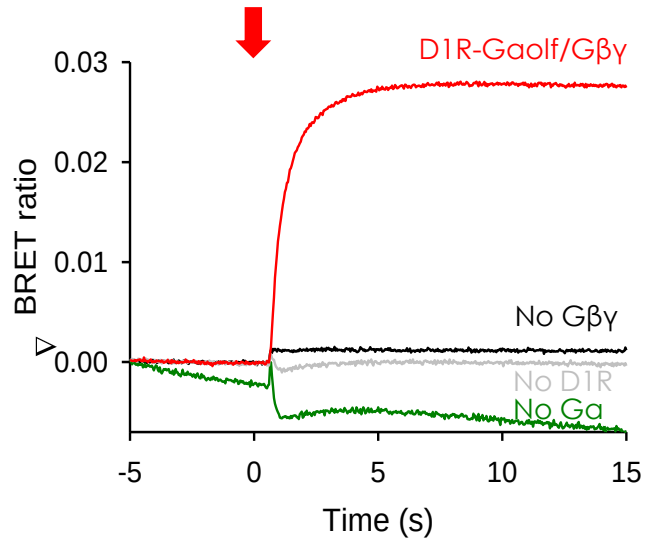

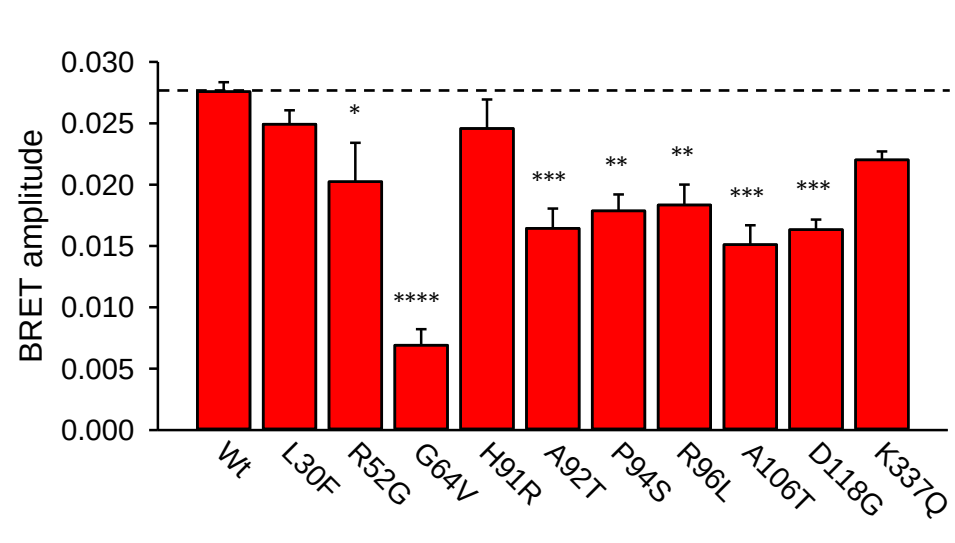

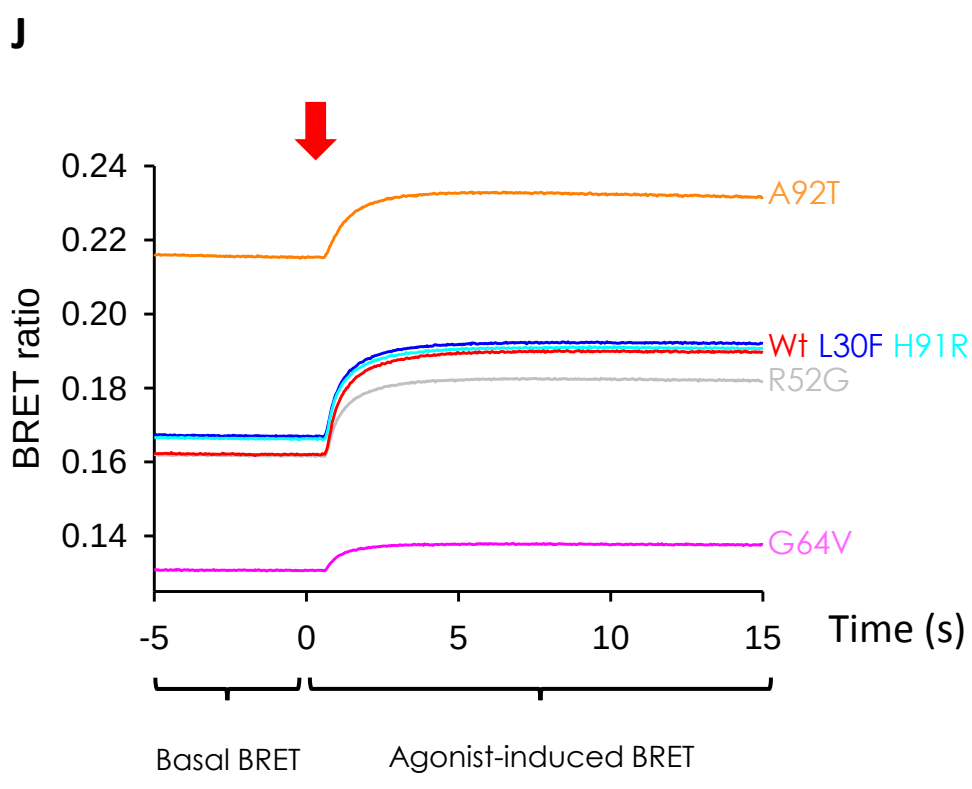

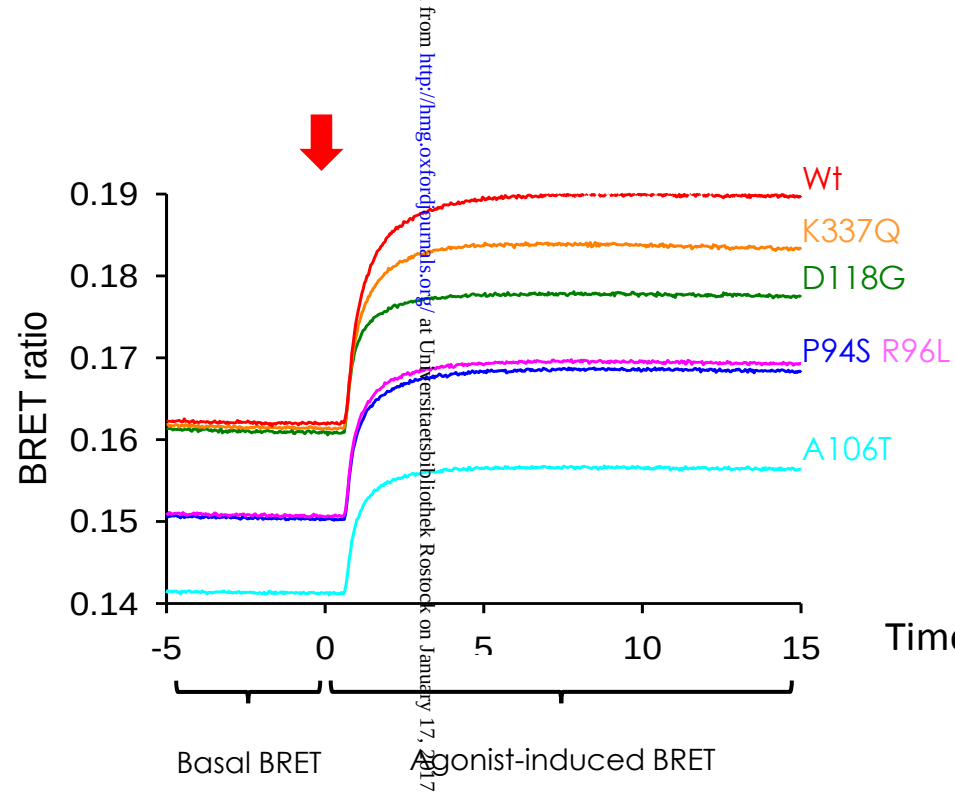

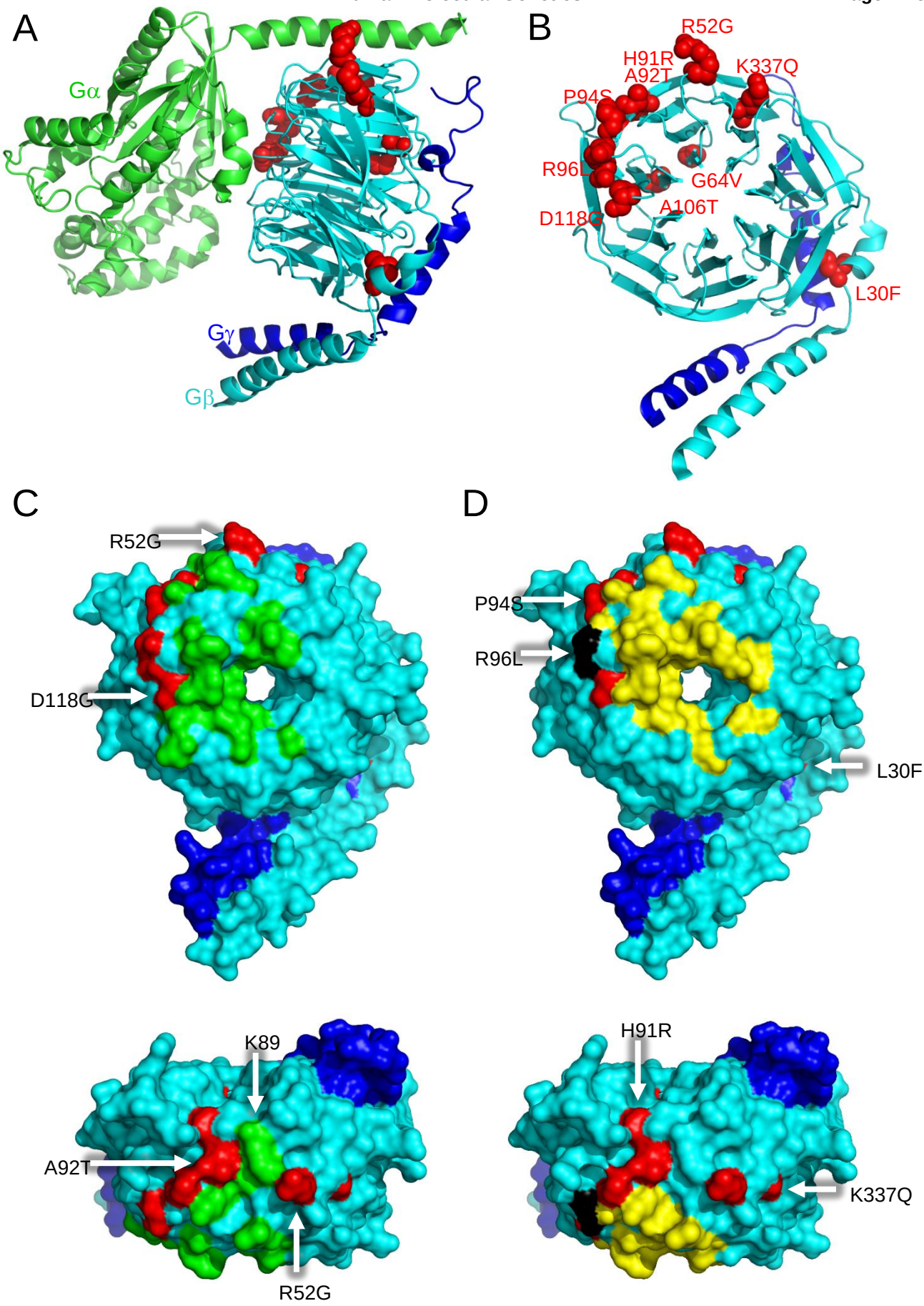
A
Gα
Gγ
Gβ
B
R52G
H91R
A92T
K337Q
P94S
R96L
G64V
A106T
D118G
L30F
C
R52G
D118G
K89
A92T
R52G
D
P94S
R96L
L30F
H91R
K337Q

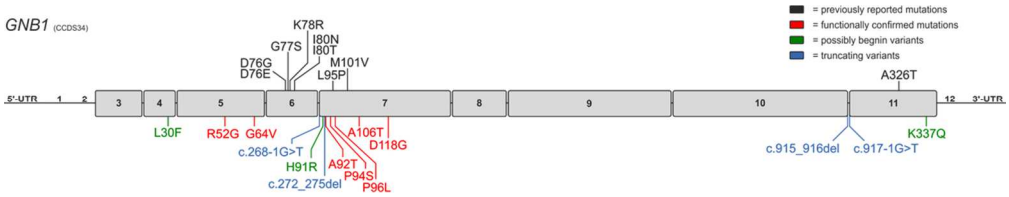

Figure 1. Schematic representation of GNB1 variants. The exons of the GNB1 gene are shown to scale with the nine coding exons highlighted by boxes and flanked by the respective untranslated regions (UTR). Previously reported mutations (2) are shown above the gene in black and newly identified variants in this study are indicated below the gene including truncating mutations (blue), missense changes which alter the functionality of Gβ1 (red), and likely benign variants (green).

338x190mm (96 x 96 DPI)

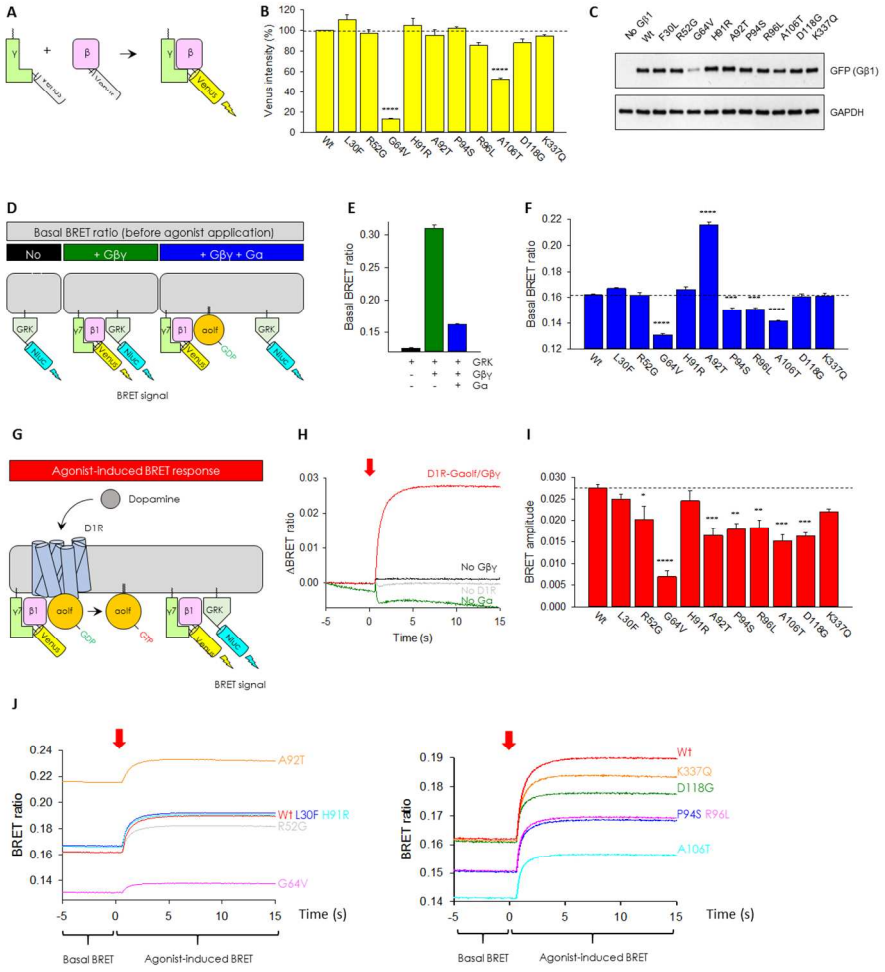

Figure 2. Effect of missense mutations in Gβ1 on Gβγ dimer formation, trimeric Golf formation and agonist-induced G protein activation.

338x451mm (96 x 96 DPI)

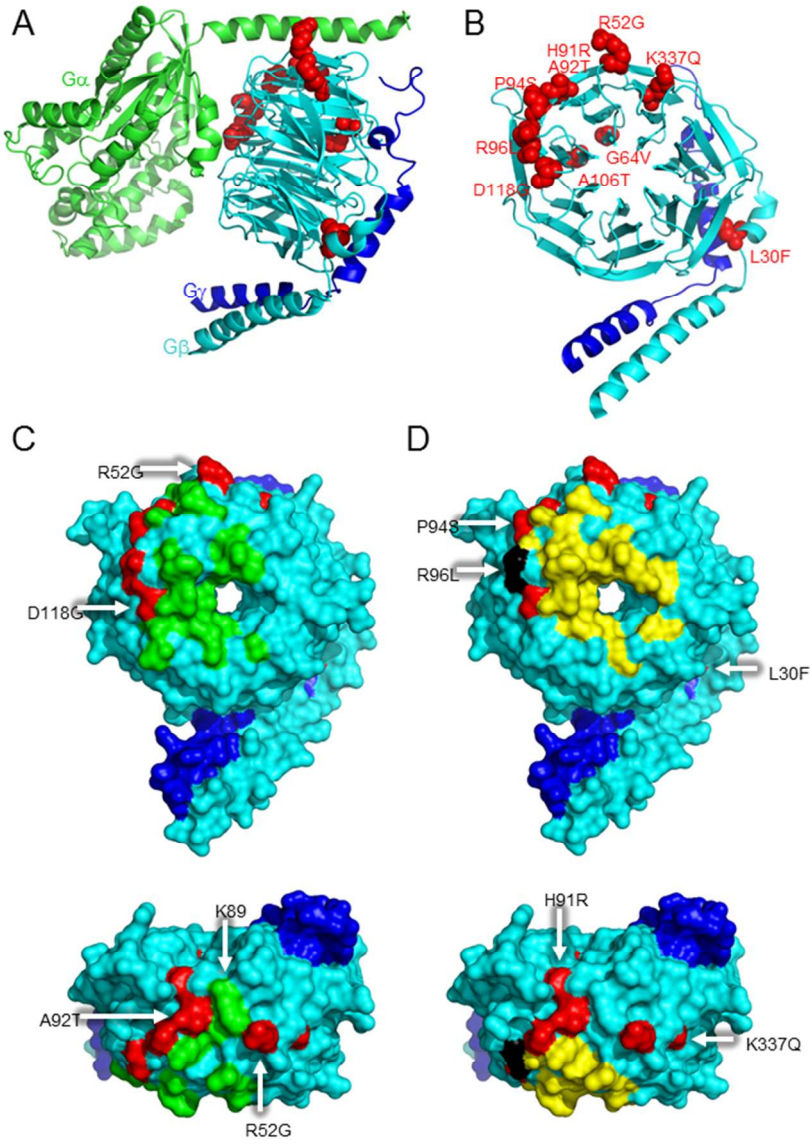

Figure 3. Mutant residues of Gβ1 on three-dimensional crystal structures. A. Cartoon representation of crystal structure of the Gαβγ trimer complex with mutations shown in red spheres. Gα, Gβ and Gγ are shown in green, cyan, and blue, respectively. The published crystal structure of Gαi1/Gβ1γ2 (PDB ID: 1GP2) was chosen as a model of the trimer (16). B. Mutant residues in Gβ1γ2 dimer found in dystonia patients are highlighted and labeled by red spheres. C and D. Binding sites on the molecular surface of Gα (C, green) and GRK (D, yellow) and on Gβ1 (cyan), respectively. Mutations are indicated in red. GRK2-Gβ1γ2 complex (PDB ID: 1OMW) (15) and Gαi1β1γ2 (PDB ID: 1GP2) were used to obtain the footprints. The residue colored in black indicates the overlap residue of the GRK binding site and the R96L mutation. The bird´s eye perspectives are shown at the bottom panels.

190x254mm (96 x 96 DPI)